Non-equilibrium of charged particles in swarms and plasmas—from binary collisions to plasma effects

2017 Plasma Phys. Control. Fusion 59 014026

(http://iopscience.iop.org/0741-3335/59/1/014026)

IOP Publishing Plasma Physics and Controlled Fusion
Plasma Phys. Control. Fusion **59** (2017) 014026 (9pp) doi:10.1088/0741-3335/59/1/014026

Non-equilibrium of charged particles in swarms and plasmas—from binary collisions to plasma effects

Z Lj Petrović[1,2], I Simonović, S Marjanović[1], D Bošnjaković[1], D Marić[1], G Malović[1] and S Dujko[1]

[1] Institute of Physics, University of Belgrade, POB 68, 11080 Zemun, Belgrade, Serbia
[2] Serbian Academy of Sciences and Arts, 11001 Belgrade, Serbia

E-mail: zoran@ipb.ac.rs

Received 23 July 2016, revised 12 September 2016
Accepted for publication 22 September 2016
Published 2 November 2016

Abstract

In this article we show three quite different examples of low-temperature plasmas, where one can follow the connection of the elementary binary processes (occurring at the nanoscopic scale) to the macroscopic discharge behavior and to its application. The first example is on the nature of the higher-order transport coefficient (second-order diffusion or skewness); how it may be used to improve the modelling of plasmas and also on how it may be used to discern details of the relevant cross sections. A prerequisite for such modeling and use of transport data is that the hydrodynamic approximation is applicable. In the second example, we show the actual development of avalanches in a resistive plate chamber particle detector by conducting kinetic modelling (although it may also be achieved by using swarm data). The current and deposited charge waveforms may be predicted accurately showing temporal resolution, which allows us to optimize detectors by adjusting the gas mixture composition and external fields. Here kinetic modeling is necessary to establish high accuracy and the details of the physics that supports fluid models that allows us to follow the transition to streamers. Finally, we show an example of positron traps filled with gas that, for all practical purposes, are a weakly ionized gas akin to swarms, and may be modelled in that fashion. However, low pressures dictate the need to apply full kinetic modelling and use the energy distribution function to explain the kinetics of the system. In this way, it is possible to confirm a well established phenomenology, but in a manner that allows precise quantitative comparisons and description, and thus open doors to a possible optimization.

Keywords: charged particle swarms, non-equilibrium plasma, skewness, resistive plate chambers, positron traps, Monte Carlo simulations, Boltzmann equation

(Some figures may appear in colour only in the online journal)

1. Introduction

The idea of thermodynamic equilibrium (TE) is one of the most widely used ideas in the foundations of plasma physics. Not only is TE used as a background gas, but it is also used as the plasma itself, and, further, TE is implicitly incorporated in most theories through application of the Maxwell Boltzmann distribution function. On the other hand, the idea of local thermodynamic equilibrium (LTE) in principle means that TE is not maintained, and that energy converted into the effective temperature is being used as a fitting parameter, but also that all the principles of TE still apply for the adjusted (local) temperature. It is often overlooked that TE implies that each process is balanced by its inverse process. It is difficult to envisage just exactly how this condition could be met under circumstances where most of the energy that is fed into the non-equilibrium, low-temperature discharges comes from an external electric field. The notion

of non-equilibrium is implemented very well in a wide range of plasma models, starting from fluid models and hybrid models, all the way to fully kinetic codes such as particle-in-cell (PIC) modelling.

At end of a field of ionized gases, opposite to the fully developed plasma, at the lowest space charge densities, electrons are accelerated (gain energy) from the external electric field and dissipate in collisions with the background gas. This realm is known as a swarm (swarm physics), and is often described by simple swarm models. We shall try to illustrate how and where one may employ concepts developed in low-temperature plasmas for problems that are not traditional non-equilibrium plasmas such as positrons in gases and gas-filled traps, gas breakdown and particle detectors.

The three selected examples are: the use and properties of higher-order transport coefficients (skewness) and how they may be implemented to close the system of equations for modeling of atmospheric plasmas; modeling of resistive plate chamber (RPC) particle detectors with a focus on the development of avalanches, and prediction of the current and deposited charge; and, finally, modeling of a generic representation of the three stage gas-filled positron trap, where the same models as for electrons may be employed in a full kinetic description to calculate the temporal development of the energy distribution function, and, through that, to describe how and when individual elementary processes affect the performance of the trap.

This is a review article as it covers three different topics that will (or have been) be presented in detail elsewhere. Yet the majority of the results will be developed in this paper. Necessarily, as it is a broad review, some finer points will be omitted in pursuit of the bigger picture, however, all will be covered elsewhere and the relevant literature is cited.

2. Higher-order transport and plasma modeling

The fluid equations often employed in plasma modeling are a part of an infinite chain, and whenever the chain is broken one needs a higher-order equation and related quantities to close the system of equations (Dujko *et al* 2013). That is why a closing of the equations is forced, sometimes labeled as ansatz, although the closure is not quite arbitrary. It is often based on some principles or simplifying arguments (Robson *et al* 2005) involving higher-order equations and related transport coefficients. Robson *et al* (2005) claimed that some serious errors have been incorporated into fluid equations that are commonly used in plasma modeling, and suggested benchmarks to test plasma models.

Equations (1) and (2) shown below, are the flux gradient equation and generalized diffusion equation, respectively, truncated at the contribution of the third order transport coefficients (also known as skewness). The terms, including $\widehat{Q}^{(\mathrm{F})}$ and $\widehat{Q}^{(\mathrm{B})}$ are terms that represent the contribution of the skewness tensor:

$$\vec{\Gamma}(\vec{r},t) = \vec{W}^{(\mathrm{F})} n(\vec{r},t) - \widehat{D}^{(\mathrm{F})} \cdot \nabla\, n(\vec{r},t) + \widehat{Q}^{(\mathrm{F})} : (\nabla \otimes \nabla) n(\vec{r},t) + \ldots \tag{1}$$

$$\frac{\partial n(\vec{r},t)}{\partial t} + \vec{W}^{(\mathrm{B})} \cdot \nabla\, n(\vec{r},t) - \widehat{D}^{(\mathrm{B})} : (\nabla \otimes \nabla) n(\vec{r},t) + \widehat{Q}^{(\mathrm{B})} \vdots (\nabla \otimes \nabla \otimes \nabla) n(\vec{r},t) + \ldots = R n(\vec{r},t) \tag{2}$$

where $\vec{\Gamma}(\vec{r},t)$, $n(\vec{r},t)$, $\vec{W}^{(\mathrm{F})}$, $\widehat{D}^{(\mathrm{F})}$, $\widehat{Q}^{(\mathrm{F})}$, $\vec{W}^{(\mathrm{B})}$, $\widehat{D}^{(\mathrm{B})}$, $\widehat{Q}^{(\mathrm{B})}$, R are the flux of charged particles, charged particle number density, flux drift velocity, flux diffusion tensor, flux skewness tensor, bulk drift velocity, bulk diffusion tensor, bulk skewness tensor and rate for reactions, respectively. If equations (1) and/or (2) are coupled to the Poisson equation for an electric field then the system of corresponding differential equations might be closed in the so-called local field approximation. This means that all transport properties are functions of the local electric field. The skewness tensor has been systematically ignored in previous fluid models of plasma discharges, although its contribution may be significant for discharges operating at high electric fields, and in particular for discharges in which the ion dynamics play an important role.

As for experimental determination of the higher-order diffusion of electrons, there have been some attempts, but those were mostly regarded as unsuccessful due to the end effects (Denman and Schlie 1990). In other words, those experiments may have failed to comply with both the requirements for negligible non-hydrodynamic regions and for lower pressures. An estimate was made that reliable skweness experiments would have to be up to 10 m long with pressures that are at least ten times smaller than those in standard swarm experiments. It seems that the only reliable yet very weak result was observed for H_2 in time of flight (TOF) emission experiments of Blevin *et al* (1976, 1978), as described in the PhD thesis by Hunter (1977). This is because the measurement was made away from the electrodes, thus providing a hydrodynamic environment.

At the same time some calculations were performed based on the available cross sections either by using a Monte Carlo simulation (MCS) and two term solutions of the Boltzmann equation (BE) (Penetrante and Bardsley 1990) or by using the momentum transfer theory (Vrhovac *et al* 1999). Whealton and Mason (1974) were the first to determine the correct structure of the skewness tensor in the magnetic field free case. For ions there have been more general studies and in particular theoretical studies. Koutselos gave a different prediction of the structure and symmetry of the tensor (Koutselos 1997) but those results were challenged (corrected) by Vrhovac *et al* (1999), who confirmed the structure of the skewness tensor previously determined by Whealton and Mason. Subsequently Koutselos confirmed the structure of the skewness tensor obtained by previous authors (Koutselos 2001).

Finally, having in mind the need for data in fluid modeling and the poor likelihood of experimental studies in the near future, a systematic study has been completed by Simonović *et al* (2016) dealing with the symmetry by using the group projector method (Barut and Raczka 1980, Tung 1984), multi-term Boltzmann equation solutions and MCS results in general terms. It should be noted that the third-order transport coefficients are often called skewness, but in principle it is the term that was to be applied only for the longitudinal diagonal

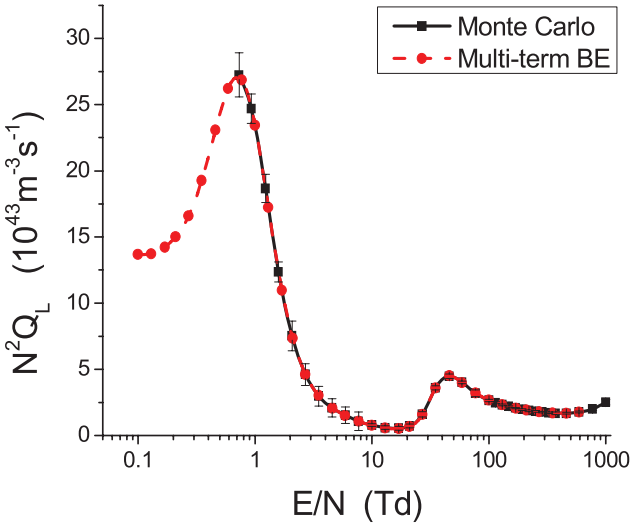

Figure 1. The longitudinal component of the skewness tensor calculated for electrons in methane.

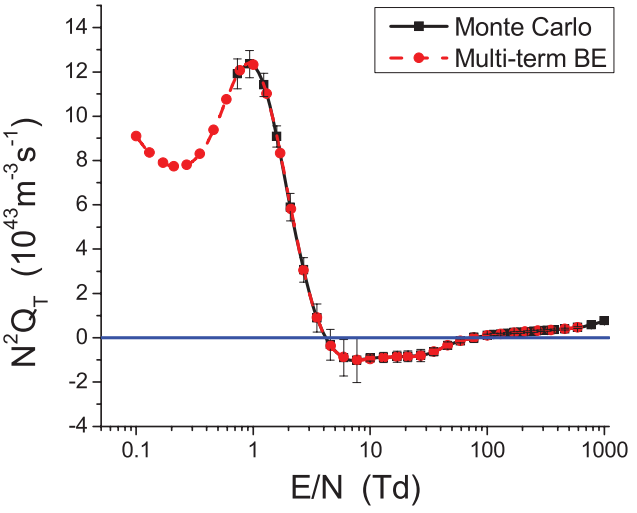

Figure 2. The transverse component of the skewness tensor calculated for electrons in methane.

term, which defines most directly the (departure from the) shape of the moving Gaussian. We will, however, use the term skewness for the entire tensor and all its terms.

The structure of the skewness tensor is the following (Whealton and Mason 1974, Vrhovac *et al* 1999, Koutselos 2001, Simonović *et al* 2016):

$$Q_{xab} = \begin{pmatrix} 0 & 0 & Q_{xxz} \\ 0 & 0 & 0 \\ Q_{xxz} & 0 & 0 \end{pmatrix}, \quad Q_{yab} = \begin{pmatrix} 0 & 0 & 0 \\ 0 & 0 & Q_{xxz} \\ 0 & Q_{xxz} & 0 \end{pmatrix}$$

$$Q_{zab} = \begin{pmatrix} Q_{zxx} & 0 & 0 \\ 0 & Q_{zxx} & 0 \\ 0 & 0 & Q_{zzz} \end{pmatrix},$$

where $a, b \in \{x, y, z\}$ and Q_{abc} are the independent, non-zero terms in the tensor (although some of them may be identical if they are established for different permutations of the same derivatives). The components of the tensor may be grouped as longitudinal $Q_{\mathrm{L}} = Q_{zzz}$ and transverse $Q_{\mathrm{T}} = \frac{1}{3}(Q_{zxx} + Q_{xxz} + Q_{xzx})$.

In this paper, we present results for skewness of electron swarms in methane. Methane is known for producing negative differential conductivity (NDC) and in this work we will demonstrate the unusual variation of the longitudinal and transverse components of the skewness tensor for *E/N* (electric field over the gas number density) regions in which NDC occurs. NDC is characterized by a decrease in the drift velocity despite an increase in the magnitude of the applied reduced electric field. Cross sections for electron scattering in methane are taken from Šašić *et al* (2004). For the purpose of this calculation we assumed a cold gas approximation: $T = 0\,\mathrm{K}$, which is justified as we covered mostly the *E/N* range where mean energies are considerably higher than the thermal energy. The initial number of electrons in the simulations was 10^7 and those were followed for sufficient time to achieve full equilibration with the applied field before sampling was applied. Sampling in an MCS is performed either for the flux (velocity space) $Q^{(\mathrm{f})}_{abc} = \frac{1}{3!}\left\langle \frac{\mathrm{d}}{\mathrm{d}t}(r^*_a r^*_b r^*_c) \right\rangle$ or for the bulk (real space) $Q^{(\mathrm{b})}_{abc} = \frac{1}{3!}\frac{\mathrm{d}}{\mathrm{d}t}\langle r^*_a r^*_b r^*_c \rangle$ components (Simonović *et al* 2016) where $r^*_a = r_a - \langle r_a \rangle$.

Uncertainties are established as the root mean square deviations. Statistical fluctuations in MCSs are more pronounced for skewness than for the lower-order transport coefficients. Thus, it is very important to present statistical uncertainties (errors) associated with the results. In addition to Monte Carlo results, the skewness tensor is calculated from the multi-term Boltzmann equation solution. The explicit formulas for skewness tensor elements in terms of moments of the distribution function will be given in a forthcoming paper (Simonović *et al* 2016).

In figures 1 and 2 we show the variation of the longitudinal and transverse skewness tensor components with *E/N* for electrons in CH_4, respectively. In figure 3 we show the variation of independent components of the skewness tensor with *E/N*. The independent components of the skewness tensor have been calculated from a multi-term solution of the Boltzmann equation.

The first observation that is very important is that the multi-term Boltzmann equation results agree very well with those obtained in MCSs. This is an important cross check and it means that the techniques to calculate the skewness are internally consistent, although two very different approaches are implemented (having said that we assume that the solution to the Boltzmann equation and the MC are both well established and tested (Dujko *et al* 2010)).

We see that Q_{T} becomes negative in the same range of *E/N* where NDC occurs. At the same time Q_{L} remains positive. Q_{zxx} and the sum of Q_{xxz} and Q_{xzx} are negative in different regions of *E/N*.

Comparing the second- and third-order longitudinal transport coefficients we noticed that if diffusion decreases with increasing *E/N* then the skewness also decreases, but even faster (figures 4 and 5). When it comes to the effect of the cross sections (or inversely to the ability to determine the cross sections from the transport data) it seems that skewness has a

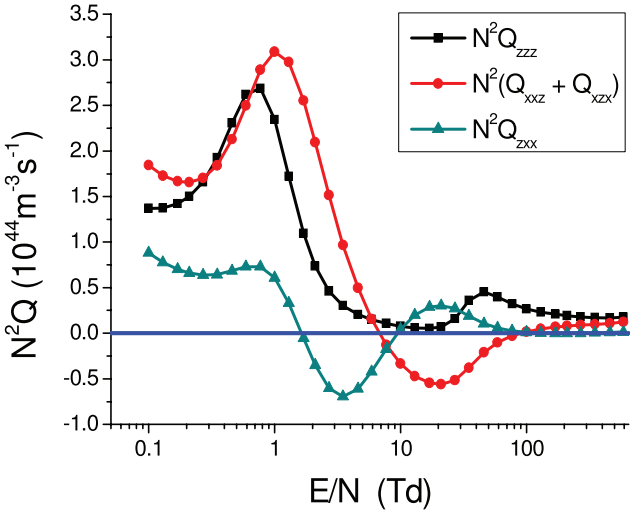

Figure 3. All independent components of the skewness tensor calculated for electrons in methane.

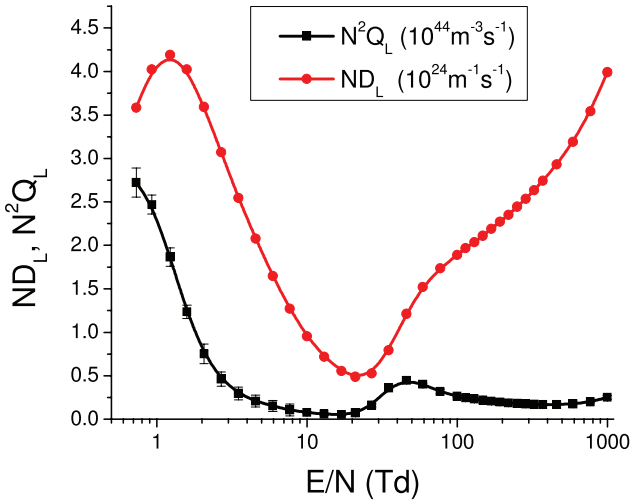

Figure 4. Comparison between longitudinal diffusion and skewness for electrons in methane (the scale for the two different transport coefficients are provided in the legend).

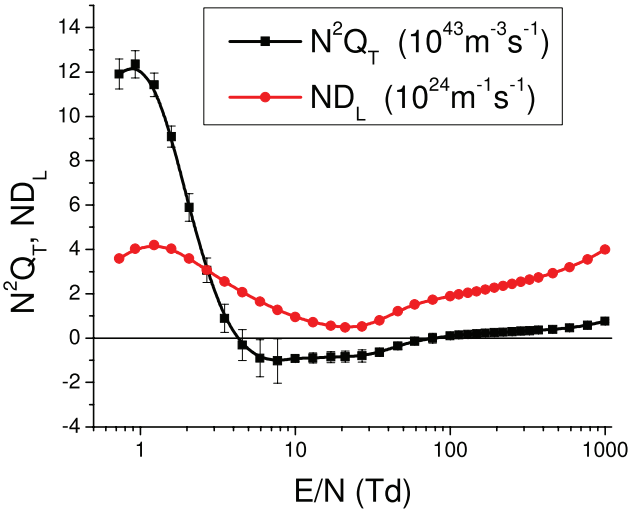

Figure 5. Comparison between longitudinal diffusion and transverse skewness for electrons in methane (the scale for the two different transport coefficients are provided in the legend).

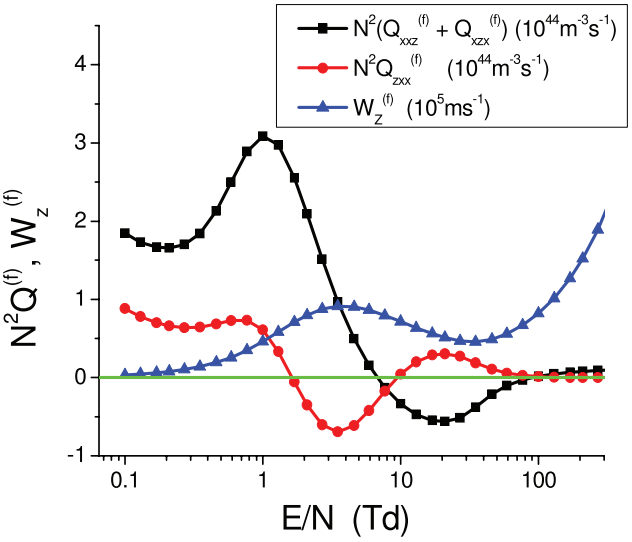

Figure 6. Off-diagonal components of skewness compared to the drift velocity for electrons in methane (the scale for the two different transport coefficients are provided in the legend).

more pronounced structure, and thus is more useful in fixing the shape and absolute values of the cross sections. If the diffusion increases, then we are able to distinguish between the two scenarios: if diffusion increases as a concave function, then the skewness decreases, while if the diffusion increases as a convex (or linear) function then the skewness increases.

We have observed that the transverse skewness is also in a good, if not better, correlation with the longitudinal diffusion (figure 5). This is a good example that illustrates that the skewness tensor represents directional motion.

Different transverse components have different *E/N* profiles. Q_{zxx} follows the behavior of the drift velocity while the remaining components change their trends of behavior near the end of the NDC region (figure 6). For different gases we have seen different trends and a clear correlation was not found (Simonović *et al* 2016).

Furthermore, but without illustrating it with special figures, the explicit effect of non-conservative collisions (ionization in this case) has been observed. However, in many cases the agreement between multi-term BE results and those obtained in MCSs is better than what would be expected based on the estimated errors. At the same time it turned out that discrepancies between a two-term and multi-term (MCS) results may be quite large, ranging up to a factor of 10.

Possible measurements of higher-order transport coefficients seem possible and also profitable for the sake of determining the cross sections. Nevertheless the difficulties and possible uncertainties may outweigh the benefits. Thus, calculation of the data seems like an optimum choice for application in higher-order plasma models. The behavior of higher-order transport coefficients provides an insight into the effect of individual cross sections (their shape and magnitude), and their features such as the Ramsauer Townsend effect or resonances on the overall plasma behavior. The transport coefficients as an intermediate step give a guidance, especially when they develop special features (kinetic effects

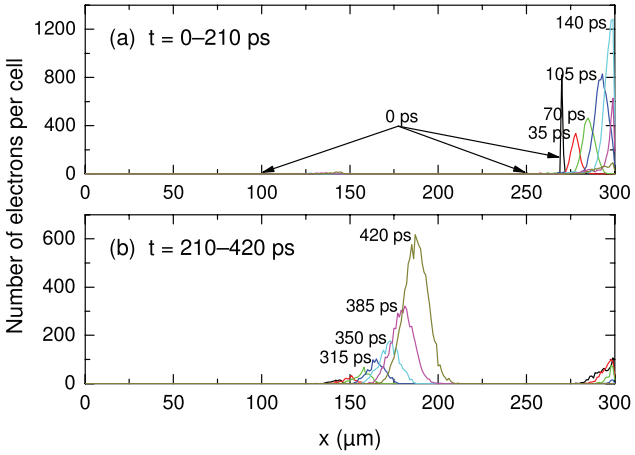

Figure 7. The spatio-temporal development of electron avalanches ((a) and (b)) in an RPC device. The number of electrons per cell (1D integration of a 3D simulation) is shown where the cells (1 cell = 1 μm) are along the discharge axis x. The cathode corresponds to $x = 0$ while the anode corresponds to $x = 300$ μm.

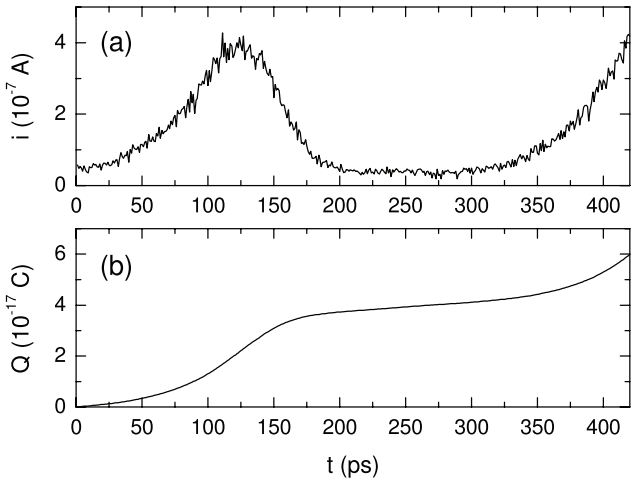

Figure 8. The time development of (a) electron induced current and (b) induced charge in the RPC device.

(Petrović *et al* 2009)) that may also be easily implemented in the determination of the cross sections.

3. Avalanches in resistive plate chambers

The next example of the connection of the elementary processes to plasma behavior through intermediate swarm-like phenomenology modeling will be modeling of RPC detectors. These devices are used for timing and triggering purposes in many high-energy physics experiments at CERN and elsewhere (The ATLAS Collaboration 2008, Santonico 2012). RPCs may be both used for spatial and temporal detection while providing large signal amplifications. They are usually operated in avalanche (swarm) or plasma (streamer) regimes depending on the required amplification and performance characteristics. Numerous models have been developed to predict RPC performance and modes of operation (Lippmann *et al* 2004, Moshaii *et al* 2012). We have studied systematically the swarm data (Bošnjaković *et al* 2014a) and then the

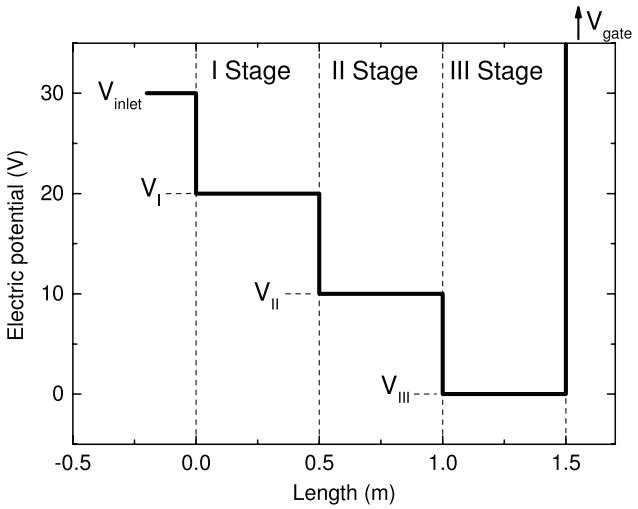

Figure 9. Schematic drawing of a generic Surko trap consisting of three equal potential drops. The composition of the background gas, its pressure and geometry are given in table 1.

Table 1. Parameters for simulation of a generic positron Surko trap.

Parameters	Stage I	Stage II	Stage III
Radius (mm)	5	20	20
Length (m)	0.5	0.5	0.5
Pressure (Torr)	10^{-3}	10^{-4}	10^{-5}
Background gas	N_2	N_2	$N_2^{0.5} + CF_4^{0.5}$
Magnetic field (G)	530	530	530
Voltage (V)	20	10	0
The initial parameters			
Potential of the entrance electrode (V)		30	
Potential of the source (V)		0.1	
Width (FWHM) of the initial energy distribution (eV)		1.5	

model of RPCs (Bošnjaković *et al* 2014b) where RPC efficiency and timing resolution have been predicted by MCS without any adjustable parameters, and were found to agree with experiment very well. Here we show some of the data not presented in Bošnjaković *et al* (2014b), which focuses on avalanche development and furthermore the induced current and charge.

Calculations of the development of the Townsend avalanche have been performed for a timing RPC gas mixture of $C_2H_2F_4$:i-C_4H_{10}:SF_6 = 85:5:10 with realistic chamber geometry (gas gap = 0.3 mm) at $E/N = 421$ Td. We show in figure 7 the development of an avalanche in the gap with three initial clusters of charges (first generation secondary electrons indicated by arrows at 0 ps) formed by an incoming high-energy particle. The first cluster (from the left) has one electron, the second has nine and the third has 983 initial electrons. The distribution over a small group of cells has been randomly selected according to well-established distributions. At the beginning, the initial condition shapes the profile of the ensemble, but eventually a Gaussian is formed that drifts under the influence of an electric field and diffuses due to numerous collisions.

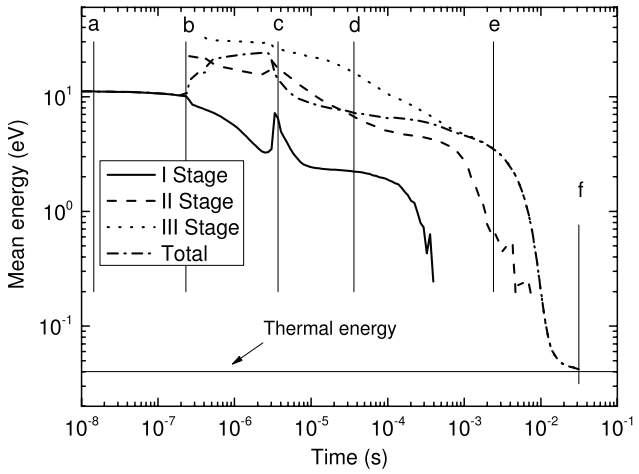

Figure 10. The mean energy of the positron ensemble (swarm) as a function of time. Averages for each stage and for the entire volume (total) are provided. The energy distribution function is plotted in figure 11 for the times marked by the points (a)–(f) in this figure.

We will first follow the development of the cluster closest to the anode (at 270 μm), as indicated by spatial electron profiles at different times in figure 7(a). The largest initial group, which is also the closest to the anode, develops the fastest: from the initial very sharp profile it quickly establishes a Gaussian shape that also very quickly gets absorbed by the anode. The second peak (from the right) is quick to follow but it is very small and cannot be observed clearly due to interference from the first pulse. In figure 7(b), we show the development of the first cluster (at 100 μm) for longer times. This cluster is the furthest from the anode and it takes the most time to reach the anode, again as a well developed moving Gaussian. It develops, however, a well-separated and defined current pulse (unlike the second cluster of charged particles). The induced current and the corresponding induced charge are shown in figure 8.

The predictions in figure 8, extended to provide important information on the temporal resolution, may be used to optimize the device by changing gas composition, field and geometry, and also may be extended to allow for the formation of the plasma in later stages when a streamer discharge may be generated at atmospheric pressure (Bošnjaković *et al* 2016). Trial and error development of such devices is simply too costly to allow for an empirical learning curve. Nevertheless, one could argue that it could be possible to develop a model based on a standard swarm description of a moving Gaussian with drift and diffusion plus the benefit of multiplication through ionization. All of these processes have their swarm coefficients. However, the very short times of the formation of the initial cluster, it being inhomogeneous and a very nonlinear growth with a possible separation of faster and slower electrons, dictate the need to perform an MCS in order to achieve the required accuracy. Thus, this example allows for the use of transport coefficients, but is better accomplished by full kinetic modeling. Transport coefficients are better taken advantage of in fluid modeling of the possibly developing streamer (Bošnjaković *et al* 2016). In any case, the ionized gas and the developing plasma channel are both represented very accurately (qualitatively and quantitatively). Here we have used kinetic swarm modeling, although using transport coefficients may also be an option, albeit a less accurate option.

4. Gas-filled positron (and electron) traps

While it is often assumed that keeping the antimatter away from the matter is a way of preserving it longer, the introduction of background gas to the vacuum magnetic field trap led to the birth of the so-called Penning Malmberg Surko traps (often known simply as Surko traps). These devices take advantage of the very narrow region of energies, where in nitrogen electronic excitation can compete and even overpower the otherwise dominant (for almost all other gases and inelastic processes) positronium (Ps) formation (Murphy and Surko 1992, Cassidy *et al* 2006, Clarke *et al* 2006, Sullivan *et al* 2008, Marjanovic *et al* 2011, Danielson *et al* 2015). To be fair, the principles of the trap have been worked out in great detail, but mostly based on beam-like considerations (Murphy and Surko 1992, Charlton and Humberston 2000). However the device consists of a charge being released in a gas in the presence of electric and magnetic fields, and thus it is an ionized gas that is exactly described by a swarm model until the space charge effects begin to play a significant role, and then it is best described by a plasma model (again with a significant reference to collisions and transport). Thus, for quantitative representation and accurate modeling of traps, a swarm-like model is required and recently two such models were used to explain the salient features of Surko traps (Marjanović *et al* 2011, Petrović *et al* 2014, Natisin *et al* 2015). An explanation and quantitative comparisons will be the subject of a specialized publication (Marjanović and Petrović 2016). Here we only focus on the development of the energy distribution function, which is the primary medium connecting the large-scale behavior of the trap with microscopic binary collisions.

As pressures used in the gas-filled traps are very low, and the mean free paths become comparable to the dimensions of the trap, one may be assured that the description at the level of transport coefficients and fluid models would fail. This example thus requires a full kinetic level of description.

The generic (model) trap consists of three stages, each with a 10 V potential drop and each of the same length (figure 9). The properties, the pressures and other features are listed in table 1. A standard, well-tested (for electron benchmarks—Lucas and Saelee 1975, Reid 1979, Ness and Robson 1986, Raspopović *et al* 1999) Monte Carlo code has been used here. Realistic geometry was included along with the boundary conditions (potentials, energy distributions and losses). Special care was given to the testing of the modeling of trajectories in magnetic fields (Raspopović *et al* 1999 Dujko *et al* 2005).

First results are shown in figure 10 where we plot mean energies as a function of time in three separate stages (chambers) and also averaged for the entire volume. The energy steps provided by the potential drops are observable for the mean energies in stages II and III. The overall increase in energy is also observed in the total volume average. The initial plateau of the mean energy is extended mainly due to

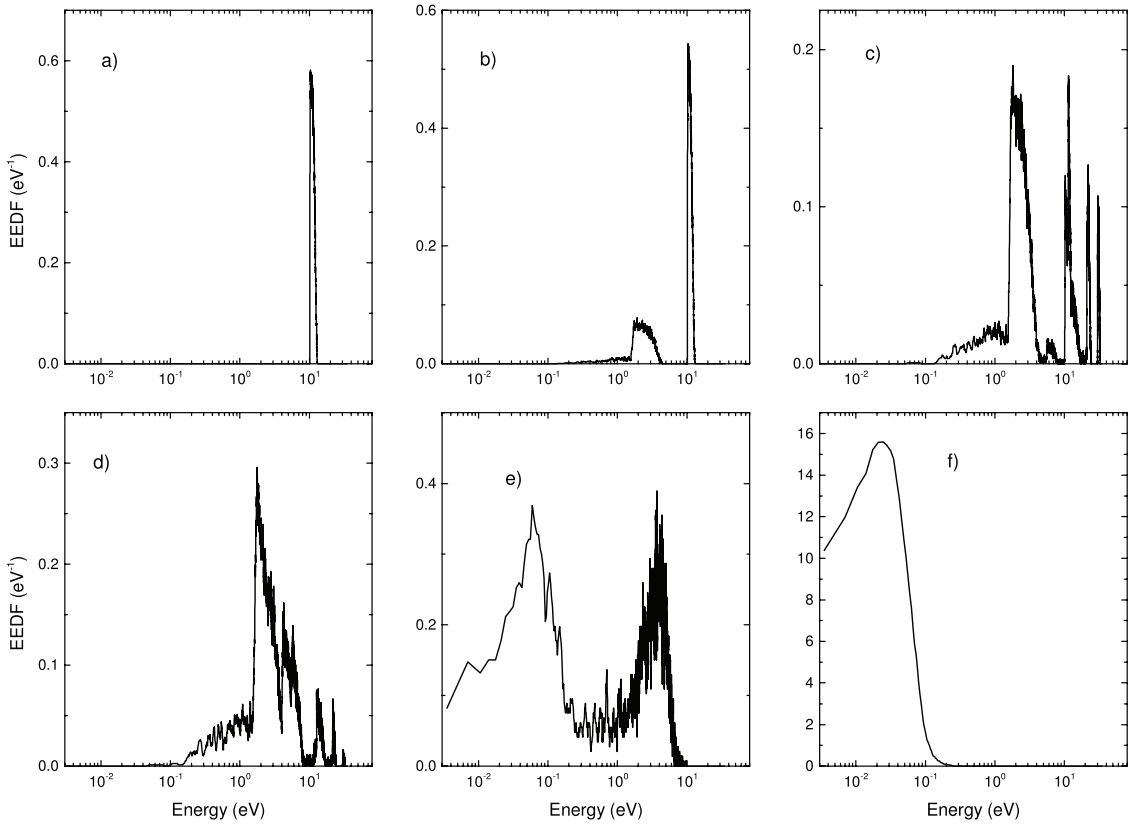

Figure 11. Positron kinetic energy distribution of the entire swarm sampled at different times (indicated in figure 10). Calculations were performed for the Surko trap as shown in figure 9 with the conditions listed in table 1.

the logarithmic nature of the plot. Following another plateau due to inelastic energy losses, the mean energy falls to the thermal value for the final thermalization.

The voltage drop in the initial stage is used to accelerate the positrons coming from the moderator into the energy range where electronic excitation of nitrogen is as efficient as Ps formation. Thus the initial distribution in figure 11 is a mono-energetic beam at 10 eV. Upon development of the group of positrons that have lost energy in excitation (figure 11(b)), positrons leave the stage I and pass into stages II and III so the two new peaks develop at 20 eV and 30 eV (figure 11(c)). The positrons that have collided form a group peaking at around 2 eV. During the next period two processes are obvious. The first is the quenching of the initial beams into the group, peaking at around 2 eV but extending up to 7 eV, where Ps formation removes the particles. The second is the process that uses vibrational excitation of CF_4 and thermalizes the 2 eV group into a low-energy group peaking at around 0.07 eV (figures 11(d) and (e)). It is interesting to see that the peak at around 2 eV is the first to disappear, leaving a group at around 5 eV to thermalize more slowly. At this point the low-energy positrons are also mainly localized in the third stage.

The final stage is characterized by two processes, the disappearance of the higher-energy group at around 5 eV and the gradual thermalization of the low-energy group at around 70 meV towards the thermal energy (f) of around 40 meV. At that point a quasi-thermal Maxwellian is developed. The transition appears to be rapid but, by the virtue of a logarithmic plot, it is the longest transition in the process of thermalization and involves bouncing between the potential boundaries of the third stage many times. At the same time one should see that the properties of the trap are adjusted so that in the first bounce across the three stages most particles suffer electronic excitation/Ps formation collisions and either disappear or are trapped.

The simulation provides many different properties of the positron ensemble (swarm) but the point of this paper is to show a direct connection between binary collision processes and the macroscopic behavior. Using the energy distribution one can easily see the dominant processes and predict which aspects of the processes are promoted by the clever design of the Surko trap. It may also be used to optimize its characteristics (Marjanović *et al* 2016). Nevertheless, the principles of the trap were properly understood from the initial concepts but in this case we have detailed representation of the energy distribution, allowing accurate quantitative comparisons. For example, one may now adjust the details of the cross section in order to fit the measured properties (such as sampled mean energy that may be somewhat skewed by the sampling process). In that respect the measured observables from the trap may play a role in the swarm data that need to be fitted in order to tune the cross sections so that the number, momentum and energy balances may be preserved. As analysis of the positron swarm data led to a number of complex kinetic effects (Banković *et al* 2009, 2012) it would be interesting to see whether similar effects may be observed or even affect the operation of the traps.

These results are akin to the well-established initial equilibration for electrons in gases (Dujko *et al* 2014) with

temporal and spatial Holst Oosterhuis luminous layers (Hayashi 1982, Fletcher 1985) that are strongly related to the well-known Frank Hertz experiment (White *et al* 2012, Robson 2014). In addition, it must be noted that even if we were to start simulation with a Maxwellian distribution and try to follow the thermalization, due to the sharp energy dependence of the processes non-Maxwellian distribution function, it would develop immediately making it necessary to employ a full kinetic treatment. While fluid equations will not work well under the circumstances, and while transport coefficients may be difficult to define and even more difficult to implement in modeling, kinetic (Monte Carlo) modeling is still a typical swarm-like model that needs to be employed. Once we fill the trap with sufficient charge to allow for plasma effects, then we may need to add-in true plasma modeling based on fluid equations and on the calculation of the effective fields.

5. Conclusion

In this review we address three recent examples on how swarm based modeling may connect the microscopic binary processes to the macroscopic behavior of ionized gases, even plasmas. The necessary prerequisite for this approach to be effective is that the systems belong to the so-called collisional plasmas (also known as the non-equilibrium or low-temperature plasmas). The examples are chosen to reveal three different aspects of swarm modeling: (a) that based on transport coefficients and fluid models and how they may be improved, (b) a system that may be described by both fluid models and simulations where simulations are used here to verify the more basic modeling, while the fluid modeling is allowing us to extend predictions further to plasma conditions, and, finally, (c) for the situation where full kinetic modeling is required. Thus, these examples should be viewed as confirmation of the validity and usefulness of the swarm models that are often overlooked by plasma modelers. Swarm models are sometimes regarded as a limit that is unrealistic and useful only to describe well-designed experiments that provide swarm data. One subscribing to that view would then need to reply to why the use of swarm data and also swarm data based fluid equations is so successful. In fact, we believe that often an 'overkill' is performed by using plasma models to describe inherently swarm-like conditions. One such example is the popular modeling of breakdown by PIC of hybrid codes. If done properly, it is all fine, although less transparent due to a more complex nature of the codes. However, at the same time such complexity does not allow us to add special tests or sampling that may reveal more insight into the pertinent physical processes. Examples may include details of the energy distribution function, adjusting boundary conditions to include detailed representation of surface processes and observation and inclusion of the kinetic phenomena.

In doing modeling of low-temperature plasmas that may need to go both more towards the swarm-like and plasma conditions we would strongly recommend that all the plasma codes need to be verified against swarm benchmarks and include sampling of relevant data. It all may become more and more difficult as one develops codes for inhomogeneous systems with complex geometry, but in the limit of a simple geometry and simple swarm conditions all swarm benchmarks should be satisfied to the highest of accuracy.

This article may be viewed as an extension of an article that has been recently submitted for a special issue on plasma modeling covering physical situations where swarm type models are valid and useful and accurate. There is no overlap of the two papers, although a common idea of the need to present the usefulness of the swarm model is obvious. The focus here is more on how elementary processes are producing an intermediate realm of phenomenology (swarm models and properties) that then clearly point at the macroscopic behavior. Be it sprite propagation or positron traps these connections not only reveal relevant physics, but also provide a means to tailor applications based on elementary processes and low-temperature plasmas.

Acknowledgment

This work was supported by the Grants No. ON171037 and III41011 from the Ministry of Education, Science and Technological Development of the Republic of Serbia and also by the project 155 of the Serbian Academy of Sciences and Arts.

References

Banković A, Dujko S, White R D, Marler J P, Buckman S J, Marjanović S, Malović G, Garcia G and Petrović Z Lj 2012 *New J. Phys.* **14** 035003

Banković A, Petrović Z Lj, Robson R E, Marler J P, Dujko S and Malović G 2009 *Nucl. Instrum. Methods Phys. Res.* B **267** 350–3

Barut A O and Raczka R 1980 *Theory of Group Representations and Applications* (Warszawa, PWN: Polish Scientific Publishers)

Blevin H A, Fletcher J and Hunter S R 1976 *J. Phys. D: Appl. Phys.* **9** 471

Blevin H A, Fletcher J and Hunter S R 1978 *Aust. J. Phys* **31** 299

Bošnjaković D, Petrović Z Lj and Dujko S 2014b *J. Instrum.* **9** P09012

Bošnjaković D, Petrović Z Lj and Dujko S 2016 *J. Phys. D: Appl. Phys.* **49** 405201

Bošnjaković D, Petrović Z Lj, White R D and Dujko S 2014a *J. Phys. D: Appl. Phys.* **47** 435203

Cassidy D B, Deng S H M, Greaves R G and Mills A P 2006 *Rev. Sci. Instrum.* **77** 073106

Charlton M and Humberston J 2000 *Positron Physics* (New York: Cambridge University)

Clarke J, van der Werf D P, Griffiths B, Beddows D C S, Charlton M, Telle H H and Watkeys P R 2006 *Rev. Sci. Instrum.* **77** 063302

Danielson J R, Dubin D H E, Greaves R G and Surko C M 2015 *Rev. Mod. Phys.* **87** 247–306

Denman C A and Schlie L A 1990 Nonequilibrium effects in ion and electron transport *Proc. of the 6th Int. Swarm Seminar (Glen Cove, NY, 1989)* ed J W Gallagher *et al* (New York: Springer)

Dujko S, Markosyan A H, White R D and Ebert U 2013 *J. Phys. D: Appl. Phys.* **46** 475202

Dujko S, Raspopović Z M and Petrović Z Lj 2005 *J. Phys. D: Appl. Phys.* **38** 2952–66

Dujko S, Raspopović Z M, White R D, Makabe T and Petrović Z Lj 2014 *Eur. Phys. J.* D **68** 166
Dujko S, White R D, Petrović Z Lj and Robson R E 2010 *Phys. Rev.* E **81** 046403
Fletcher J 1985 *J. Phys. D: Appl. Phys.* **18** 221–8
Hayashi M 1982 *J. Phys. D: Appl. Phys.* **15** 1411–8
Hunter S R 1977 *PhD Thesis* Flinders University, Adelaide, Australia unpublished
Koutselos A D 1997 *J. Chem. Phys.* **106** 7117–23
Koutselos A D 2001 *Chem. Phys.* **270** 165–175
Lippmann C and Riegler W 2004 *Nucl. Instrum. Methods Phys. Res.* A **533** 11–5
Lucas J and Saelee H T 1975 *J. Phys. D: Appl. Phys.* **8** 640–50
Marjanović S, Banković A, Cassidy D, Cooper B, Deller A, Dujko S and Petrović Z Lj 2016 *J. Phys. B: At. Mol. Opt. Phys.* **49** 215001
Marjanovic S, Šuvakov M, Bankovic A, Savic M, Malovic G, Buckman S J and Petrovic Z Lj 2011 *IEEE Trans. Plasma Sci.* **39** 2614–5
Marjanović S and Petrović Z Lj 2016 *Plasma Sources Sci. Technol.* submitted
Moshaii A, Khosravi Khorashad L, Eskandari M and Hosseini S 2012 *Nucl. Instrum. Methods Phys. Res.* A **661** S168–71
Murphy T J and Surko C M 1992 *Phys. Rev.* A **46** 5696–705
Natisin M R, Danielson J R and Surko C M 2015 *Phys. Plasmas* **22** 033501
Ness K F, Robson R E 1986 *Transp. Theor. Stat. Phys.* **14** 257–90
Penetrante B M and Bardsley J N 1990 *Nonequilibrium Effects in Ion and Electron Transport* ed J W Gallagher *et al* pp 49–66 (New York: Plenum)
Petrović Z Lj, Dujko S, Marić D, Malović G, Nikitović Ž, Šašić O, Jovanović J, Stojanović V and Radmilović-Rađenović M 2009 *J. Phys. D: Appl. Phys.* **42** 194002
Petrović Z Lj *et al* 2014 *J. Phys.: Conf. Ser.* **488** 012047
Raspopović Z M, Sakadžić S, Bzenić S and Petrović Z Lj 1999 *IEEE Trans. Plasma Sci.* **27** 1241–8
Reid I D 1979 *Aust. J. Phys.* **32** 231–54
Robson R E, White R D and Hildebrandt M 2014 *Euro. Phys J.* D **68** 188
Robson R E, White R D and Petrović Z Lj 2005 *Rev. Mod. Phys.* **77** 1303
Santonico R 2012 *Nucl. Instrum. Methods Phys. Res.* A **661** S2–5
Simonović I *et al* 2016 unpublished
Šašić O, Malović G, Strinić A, Nikitović Ž and Petrović Z Lj 2004 *New J. Phys.* **6** 74–85
Sullivan J P, Jones A, Caradonna P, Makochekanwa C and Buckman S J 2008 *Rev. Sci. Instrum.* **79** 113105
Whealton J H and Mason E A 1974 *Ann. Phys.* **84** 8–38
White R D, Robson R E, Nicoletopoulos P and Dujko S 2012 *Eur. Phys. J.* D **66** 117
The ATLAS Collaboration 2008 *J. Instrum.* **3** S08003
Tung W-K 1984 *Group Theory in Physics* (Singapore: World Scientific Publishing)
Vrhovac S B, Petrović Z Lj, Viehland L A and Santhanam T S 1999 *J. Chem. Phys.* **110** 2423–30